Metabolism of Triallate in Sprague-Dawley Rats. 2. Identification and Quantitation of Excreted Metabolites

Ronn G. Nadeau,* Robert C. Chott, Hideji Fujiwara, Huey-Sheng Shieh, and Eugene W. Logusch

Monsanto Company, St. Louis, Missouri 63198

[^{13}C,^{14}C]Triallate was administered orally to Sprague-Dawley rats. Twelve excreted metabolites were identified, the most abundant being 2,3,3-trichloro-2-propenesulfinic acid. Five metabolites derived from 2,3,3-trichloro-2-propenethiol were identified in excreta, including a methyl sulfone mercapturate whose structure was confirmed by X-ray crystallography. Three 2-chloroacrylate metabolites were identified, including a 2-chloroacrylate mercapturate whose structure was confirmed by X-ray crystallography. 2,3,3-Trichloro-2-propenol and hydroxytriallate were also identified as metabolites. Dosing of radiolabeled thiol and sulfinic acid to separate animals resulted in excretion of only thiol-derived metabolites in the urine of thiol-dosed rats, while sulfinic acid and sulfonic acid were excreted by sulfinic acid-dosed rats. Triallate metabolism in rats proceeds via three main pathways, i.e., S-oxidation leading to sulfur acids, S-oxidation/hydrolysis/reduction leading to thiol derivatives, and C-oxidation of the 2,3,3-trichloropropenethiol moiety. This study demonstrates that formation of readily excreted sulfur acids and thiol derivatives is the major route of triallate metabolism in rats.

INTRODUCTION

The preceding paper in this issue (Ridley et al., 1993) describes the dosing of rats with radiolabeled triallate, as well as the kinetics of dose elimination, quantitative distribution of the dose, and characterization of the radioactivity found in blood. In this paper we report metabolites excreted by rats dosed with triallate and we propose metabolic pathways to account for the formation of these metabolites. We also describe separate feeding experiments, using radiolabeled metabolite intermediates, which allowed us to delineate the pathways of triallate metabolism in rats. The following paper (Hackett et al., 1993) presents an investigation of triallate in vitro metabolism using rat liver enzymes and provides mechanistic details for the pathways of triallate breakdown. Several other thiocarbamate animal metabolism studies have been reported (Chen et al., 1979; Debaun et al., 1978; Hubbell and Casida, 1977; Casida et al., 1975), although little information on in vivo triallate metabolism has been available (Marsden and Casida, 1982).

Triallate undergoes extensive breakdown in the laboratory rat, and twelve in vivo metabolites have been identified using a combination of techniques, including NMR spectroscopy, mass spectrometry, chemical synthesis, and X-ray crystallography. Triallate metabolites described in this paper, and derivatives thereof prepared for the purpose of structure elucidation, are shown in Figure 1. All structures are marked with an asterisk to indicate the location of isotopic labeling in the triallate test substance and in resulting metabolites. Synthetic standards (e.g., **2a**) are similarly marked for convenience.

MATERIALS AND METHODS

Chemicals. [^{14}C]Triallate labeled in the C-1 position was prepared by starting with [1-^{14}C]-1,2,3,3-tetrachloro-2-propene (New England Nuclear, Inc., Boston, MA). [^{13}C]Triallate labeled in the C-1 position was prepared by starting with [^{13}C]methyl iodide (KOR Isotopes, Cambridge, MA). Appropriate amounts of [^{12}C]-, [^{13}C]-, and [^{14}C]triallate were combined to produce test substances with specific radioactivities of 0.24 (high dose) and 4.7 mCi/mmol (low dose). The ^{13}C enrichment in both test substances was 50%. Chemical and radiochemical purities were a minimum of 98.5%. [1-^{14}C]-2,3,3-Trichloro-2-propenethiol was prepared by reaction of [1-^{14}C]-1,2,3,3-tetrachloro-2-propene with thiourea and hydrolysis of the resulting isothiuronium salt with 1 N NaOH. The product was 97% radiochemically pure and 95% chemically pure. [1-^{14}C]-2,3,3-Trichloro-2-propenesulfinic acid (**2**) was prepared by treating [^{14}C]triallate with sodium periodate and HCl in methanol to produce methyl [1-^{14}C]-2,3,3-trichloro-2-propenesulfinate (**2a**), which was hydrolyzed with

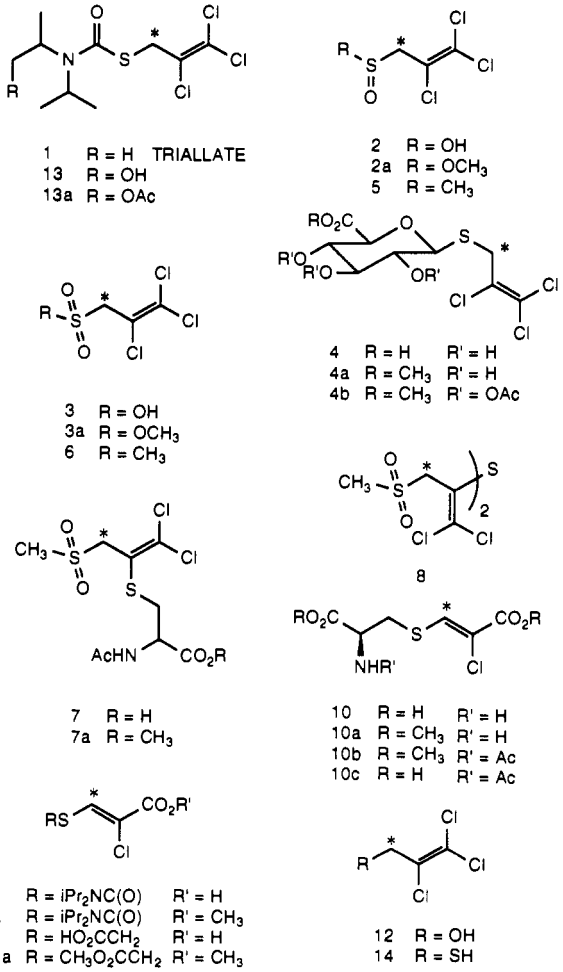

Figure 1. Triallate rat metabolites and derivatives.

0021-8561/93/1441-0132$04.00/0

NaOH, giving 2 in 31% yield. The radiochemical preparation of 2 was a scaled-down version of the method described in detail below for unlabeled 2. Radiolabeled 2 was purified by HPLC on the day of administration and had a radiochemical purity of 80%. Insta-Gel scintillation cocktail was obtained from Packard Instrument Co. (Downers Grove, IL). All other chemicals and solvents employed were of the highest purity obtainable from commercial suppliers.

Animals and Dosing. Sprague-Dawley rats were purchased from Charles River Laboratories (Wilmington, MA). The low-dose (5 mg/kg) and high-dose (500 mg/kg) groups each consisted of five male and five female rats. Details of animal care, dosing, and sample collection are described in the preceding paper (Ridley et al., 1993).

Excreta Collection and Sample Preparation. Excreta were collected at 6, 12, and 24 h after dosing, and daily thereafter for 10 days. Individual pooled urine and pooled fecal samples were prepared for each rat in each group, using 10% portions (by weight) of each time-point sample but including only time-point samples containing at least 5% of the total excreted radioactivity. Samples represented 95–98% of the radioactivity excreted by each animal. Portions of the pooled fecal samples were extracted three times with acetone/water (60/40) by shaking for 30 min, centrifuging, and decanting the supernatants. Extracts were analyzed by liquid scintillation counting (LSC) and pellets by combustion, demonstrating extraction efficiencies of 77–82%. Fecal extracts were concentrated by rotary evaporation at 25 °C to remove acetone, and both concentrates and distillates were analyzed by LSC to demonstrate the absence of significant radioactive carryover in distillates. Concentrates were centrifuged in a Dynac centrifuge (Fisher Instruments, St. Louis, MO) at full speed (1000g) for 5 min to remove particulates prior to HPLC analysis. Urine samples were likewise centrifuged prior to HPLC.

Metabolite HPLC Analysis. The HPLC equipment consisted of a Waters 680 controller and M6000 pumps (Waters Associates, Milford, MA), a Waters U6K injector equipped with a 2-mL sample loop, a Schoeffel 770 UV detector tuned to 254 nm (Waters Associates), an Altex Ultrasphere-ODS (10 mm × 25 cm) column protected with a C-18 guard column (P. J. Cobert Associates, St. Louis, MO), and an ISCO Model 328 fraction collector (ISCO Instrument Co., Lincoln, NE). The profiling HPLC gradient was conducted in linear steps at a flow rate of 4 mL/min, utilizing 1% acetic acid (solvent A) and acetonitrile (solvent B). The gradient proceeded from 5% B to 15% B over 4 min, to 30% B over 9 min, to 100% B in 7 min and remained at 100% B for an additional 10 min. HPLC eluents were collected at 0.3-min intervals in scintillation vials, Insta-Gel scintillation cocktail was added, samples were analyzed by liquid scintillation counting (LSC), and data were converted to histogram form using Monsanto LSC software (Figure 2). Histogram distribution data were combined with percentages of dose in urine and feces (Ridley et al., 1993) for calculation of metabolite distributions as percentages of dose (see Results). A Waters analytical μBondapak C-18 column was used for determining retention times of metabolites relative to that of coinjected triallate and for comparing retention times of metabolites with those of authentic standards. Analytical HPLC was conducted at a flow rate of 2 mL/min with 1% acetic acid (solvent A) and acetonitrile (solvent B). The analytical HPLC gradient proceeded from 0% B to 100% B over 20 min and was held at 100% B for 5 min. Analytical HPLC retention times of metabolites are shown in Table I.

Metabolite HPLC Isolation. Acidic metabolites (2–4, 7, 9–11) were isolated by preparative HPLC of urine samples selected for richness in the desired metabolite, using a semi-preparative Altex Ultrasphere ODS column and the same elution conditions as described for HPLC metabolite profiling. Neutral metabolites (5, 6, 8, 12, 13) were first extracted with methylene chloride from urine samples, and the residues after solvent evaporation were dissolved in acetonitrile or methanol and purified by preparative HPLC with radioactivity detection (RAD) using a Radiomatic Model BD flow-through radioactivity detector (Radiomatic Co., Meriden, CT). HPLC solvents were removed by rotary evaporation, and the residues were redissolved in methanol or acetonitrile for LSC analysis. Isolates were analyzed by analytical HPLC to determine radiochemical purity and, when necessary, were repurified by preparative HPLC prior to derivatization and/or spectroscopic analysis.

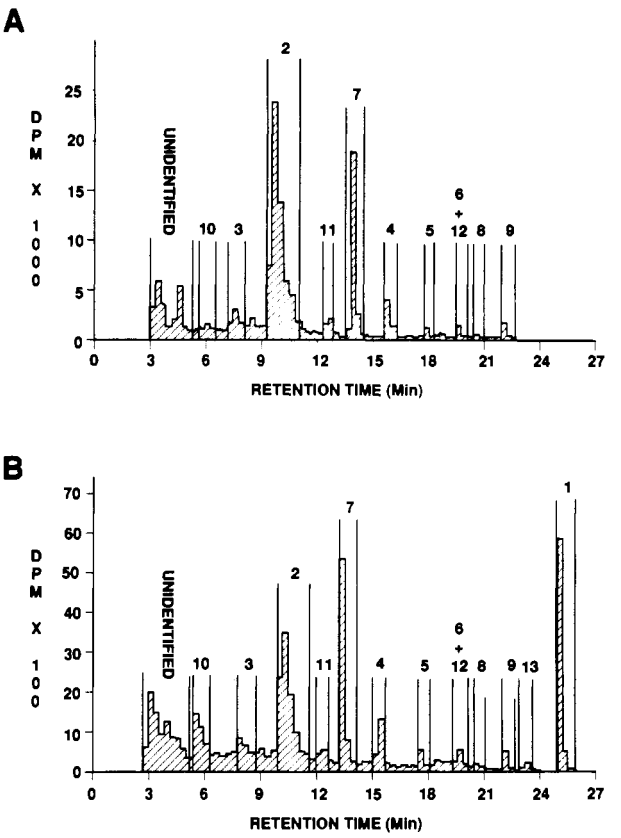

Figure 2. Representative HPLC histogram of metabolite distributions in excreta of male rats dosed at 500 mg/kg: (A) urine; (B) feces. See Materials and Methods for HPLC quantitation gradient conditions.

Table I. Analytical HPLC Retention Times of Triallate Metabolites and Derivatives[a]

structure[b]	metabolite	methyl ester	acetate	acetylated methyl ester
1	19.4			
2	7.8	12.4		
3	6.8	13.6		
4	9.5	11.1		16.3
5	10.1			
6	11.3			
7	8.7	10.1		
8	13.2			
9	14.9	17.8		
10	5.4	8.3	7.8	11.4
11	8.5	13.2		
12	11.4			
13	16.1		18.6	

[a] Analytical retention times in minutes. Analyzed with Waters μBondapak column, linear gradient of 1% acetic acid (A) and acetonitrile (B), flow rate of 2 mL/min: 0% → 100% B over 20 min, held at 100% B for 5 min. [b] See Figure 1 for structures.

Gas Chromatography (GC). GC analyses were performed on glass columns (180 cm long × 2 mm i.d.) packed with 3% OV-17 on 80–100 CW-HP support, using a Varian Series 3700 instrument equipped with a flame ionization detector and an initial program temperature of 120 °C (5 min) followed by an increase to 300 °C at 10 °C/min.

Mass Spectrometry (MS) and Nuclear Magnetic Resonance (NMR) Spectroscopy. Chemical ionization (CI) and electron impact (EI) mass spectra were obtained using a Varian MAT CH-7A single-sector mass spectrometer equipped with a jet separator interface maintained at 300 °C. Negative-ion GC/CI mass spectra were obtained on a Finnigan 4535 quadrupole instrument. High-resolution and field-desorption mass spectra were obtained using a Varian MAT 311-A double-sector instru-

Table II. Selected ^{13}C NMR Shifts of Triallate and Metabolites[a]

compd	solvent	C-1	C-2	C-3
1	$CDCl_3$	35.2	119.8	129.3
2	D_2O	67.7[b]		
2a	$CDCl_3$	63.2	121.3	123.4
3	D_2O	56.5	122.8	123.5
4	D_2O	35.1[b]		
6	$CDCl_3$	60.7	120.2	126.1
7	D_2O	57.7	121.1	130.7
10	D_2O	136.6[b]		
10c	D_2O	145.1	117.5	163.8
11	D_2O	138.6	122.8	167.4

[a] Shifts in ppm downfield from TMS. [b] Sample limitations permitted determination of C-1 shift only.

ment. All CI spectra were obtained using either isobutane or ammonia as the reagent gas, as noted. GC mass spectra were acquired and processed by an on-line mass spectral data system employing DEC 11/34 and 11/55 computers (Digital Equipment Corp., Boston, MA). Mass spectral data for metabolites and derivatives are provided in the supplementary material. High-resolution ^1H NMR spectra were obtained using a Bruker 360-MHz instrument. ^{13}C NMR data were obtained on a JEOL FX-100 spectrometer (Table II).

Liquid Scintillation Counting Analysis (LSC). LSC was performed using Insta-Gel cocktail and Mark III counters (Model 6881, TM Analytic Inc., Elk Grove Village, IL) interfaced with a PDP 11/34 computer (Digital Equipment).

X-ray Crystallography. X-ray crystal diffraction data were collected using a Syntex P21 autodiffractometer. The Enraf-Nonius structure determination package was used for data processing and structure determination and refinement. All calculations were performed on a PDP 11/34 computer.

High-Voltage Electrophoresis (HVE). HVE was performed on a Savant FP-30A flatbed instrument (Savant Instruments, Hicksville, NY) equipped with HV-10000 power supply and recirculating cooler to maintain temperatures near 10 °C. Samples were spotted on Whatman 3 MM paper (185 g/m^2; Reeve Angel Co., Clifton, NJ). HVE was typically performed at 3000 V for 30 min, using buffers of pH 5.9 (200 mL of pyridine and 30 mL of glacial acetic acid in 1800 mL of water), pH 2.0 (60 mL of 88% formic acid and 240 mL of glacial acetic acid in 2700 mL of water), and pH 1.0 (0.1 N HCl).

Derivatization Procedures. Acetylations were conducted on samples brought to dryness by rotary evaporation or by a stream of nitrogen. Typically, 100 μL of pyridine and 200 μL of acetic anhydride were added to a dry sample in a 15-mL screw-cap centrifuge tube. After capping and mixing, the tube was maintained in a water bath at 40 °C for 30–60 min. Reagents were removed using a stream of nitrogen, and the product was dissolved in an appropriate solvent for further analysis. Methyl esters were prepared by adding ethereal diazomethane in a well-ventilated hood to cooled methanolic solutions of the acid until persistence of a yellow color. Solvent was removed by a stream of nitrogen.

Sulfonate methyl ester **3a** was prepared from sulfonic acid metabolite **3** after conversion of the latter to the free acid by elution in methanol through a small prewashed cation-exchange resin column in a Pasteur pipet (2–3 cm of AG-50 X-4, H^+ form). The eluent was transferred to a thick-walled 15-mL screw-cap tube and was reduced to dryness with a stream of nitrogen. Approximately 1 mL of trimethyl orthoformate was added, and the tightly capped tube was placed in an oven at 100 °C for 1 h; **3a** was analyzed by HPLC after cooling. Sulfinic acid metabolite **2** was prepared for derivatization to methyl sulfone **6** by rotary evaporation of solvent, and the residue was transferred to a test tube using approximately 0.5 mL of 10 mM KH_2PO_4 buffer and 1–2 mL of ethanol. Methyl iodide (200 μL) was added, and the test tube was capped and placed in a water bath maintained at 45 °C. The progress of the reaction was monitored by HPLC using UV or RAD detection. Water was added after 3 h, and the mixture was extracted with methylene chloride. Methyl sulfone **6** was analyzed by mass spectrometry after the methylene chloride extract was passed through a column of anhydrous sodium sulfate in a Pasteur pipet.

Synthesis of 2,3,3-Trichloro-2-propenesulfinic Acid (2). Sodium periodate (2.63 g, 12.3 mmol) and concentrated HCl (3.08 mL, 37 mmol) were added to 200 mL of anhydrous methanol in a 1-L round-bottom flask. The reaction mixture was stirred at room temperature until all of the salt had dissolved, resulting in a pale yellow solution. The reaction solution was cooled to 0 °C, and a chilled solution of triallate (3.75 g, 12.3 mmol) in 200 mL of methanol was added. The stirred reaction mixture was allowed to warm to room temperature, with monitoring by HPLC. After 4 h, the triallate peak had disappeared and the main product peak (>90%) corresponded to the sulfinate methyl ester **2a**. The reaction mixture was poured into 400 mL of water and extracted four times with pentane. The pentane extract was washed twice with 0.5 M sodium sulfite and twice with water and was dried over magnesium sulfate. Pentane was removed by rotary evaporation from an ice-cooled flask, leaving a pale yellow oil weighing 4.48 g. ^1H NMR analysis showed that the crude product contained **2a** and byproduct methyl *N,N*-diisopropylcarbamate (methyl resonance at 1.10 ppm). Kugelrohr distillation yielded a forerun (25 °C, 2 mmHg) containing the carbamate and a small amount of **2a**. Further distillation (35 °C, 1 mmHg) afforded pure **2a** (0.837 g, 31%). The ^1H NMR spectrum of **2a** displayed methyl ester and methylene signals at 3.80 and 3.95 ppm, respectively. The ^{13}C NMR spectrum was consistent with the proposed structure (Table II). Anal. Calcd for $C_4H_5SO_2Cl_3$: C, 21.5; H, 2.26; S, 14.34; Cl, 47.59. Found: C, 21.73; H, 2.30; S, 14.23; Cl, 47.49.

A vigorously stirred, nitrogen-purged solution of **2a** (22.2 mg, 0.10 mmol) in 16 mL of methanol and 4 mL of water was cooled to 0 °C, and sodium hydroxide (1 N, 0.2 mL) was added. Analytical HPLC 1 min after addition of base indicated the absence of **2a** and the appearance of a single new product with an HPLC retention time corresponding to that of sulfinic acid **2**. The solution was transferred to a 100-mL round-bottom flask and was subjected to rotary evaporation using a 25 °C water bath and a vacuum pump (10 mmHg). The residue was treated with methyl iodide as described under Derivatization Procedures, giving the methyl sulfone **6**, which displayed a GC/EI mass spectrum essentially identical to that of **6** produced by large-scale synthesis via a different route (see below).

Synthesis of Methyl 1-Deoxy-1-[(2,3,3-trichloro-2-propenyl)thio]-β-D-glucopyranuronate (4a). Methyl glucuronate (**4a**) was synthesized via conversion of methyl triacetyloxy-β-D-glucuronate (Bowering and Timell, 1959) to the bromo sugar and reaction with 2,3,3-trichloropropenethiol (see supplementary material). HPLC-purified **4a** was treated with acetic anhydride/pyridine, and triacetate **4b** displayed a CI mass spectrum containing an $[M + H]^+$ ion cluster at m/z 493, with the heaviest ion cluster in the EI spectrum at m/z 372, $[M - (2\ CH_3CO_2H)]^+$. The ^1H NMR spectrum of **4b** showed a doublet at 4.67 ppm (J = 9 Hz) for the proton attached to the anomeric carbon, indicative of an axial configuration and therefore an equatorial (β) sulfur–carbon bond.

Synthesis of 1,1,2-Trichloro-3-(methylsulfonyl)-1-propene (6). Sulfone **6** was prepared by reaction of sodium methanesulfinate with 1,1,2,3-tetrachloropropene (see supplementary material). Synthetic **6** exhibited a GC/EI mass spectrum with an $[M]^+$ ion at m/z 222. The ^1H NMR spectrum of **6** displayed methyl ester and methylene signals at 3.05 and 4.30 ppm, respectively. Anal. Calcd for $C_4H_5Cl_3O_2S$: C, 21.5; H, 2.3; Cl, 47.6; S, 14.1. Found: C, 21.4; H, 2.3; Cl, 47.4; S, 14.1.

Synthesis of *N*-Acetyl-*S*-[2,2-dichloro-1-[(methylsulfonyl)methyl]ethenyl]-L-cysteine (7). Mercapturate **7** was prepared via reaction of sulfone **6** with *N*-acetylcysteine (see supplementary material). Single-crystal X-ray analysis of synthetic **7** showed that the mercapturate group was attached at the C-2 position (Figure 3, see Results). Anal. Calcd for $C_9H_{14}Cl_2NO_5S_2$: C, 30.1; H, 3.9; Cl, 19.7; S, 17.8. Found: C, 30.4; H, 3.9; Cl, 20.2; S, 17.9.

Synthesis of *N*-Acetyl-(*Z*)-*S*-(2-carboxy-2-chloroethenyl)-L-cysteine (10c). The mercapturate **10c** was prepared via reaction of *N*-acetylcysteine with 2,3-dichloroacrylic acid (see supplementary material). Synthetic **10c** was a crystalline solid, mp 184–187 °C, and displayed ^{13}C resonances consistent with

the expected structure (Table II). EI and CI mass spectral data for ester **10b**, produced by treatment of **10c** with diazomethane, were also consistent with the assigned structure (supplementary material).

Synthesis of (*Z*)-3-[(Carboxymethyl)thio]-2-chloro-2-propenoic Acid (11). The 2-chloroacrylate 11 was prepared via reaction of sodium mercaptoacetate with 2,3-dichloroacrylic acid (see supplementary material). Synthetic 11 displayed ^{13}C resonances consistent with the expected structure (Table II). A portion of the product was treated with diazomethane to produce methyl ester **11a**, which gave the expected mass spectral data (supplementary material).

RESULTS

Metabolite Identification. Twelve triallate rat metabolites were identified in this study and are illustrated in Figure 1 (2–13), together with prepared derivatives. Metabolite identifications are presented in an order reflecting the pathways of triallate metabolism: (1) sulfur oxidation, followed by hydrolysis and further oxidation, leading to the sulfinic acid **2** and sulfonic acid **3**; (2) sulfur oxidation, followed by hydrolysis and reduction, leading to thiol-derived products **4**–**8**; and (3) carbon oxidation leading to 2-chloroacrylates **9**–**11**, trichloroallyl alcohol **12**, and hydroxytriallate **13**.

Metabolite 2 (2,3,3-Trichloro-2-propenesulfinic Acid). Field desorption (FD) mass spectral analysis of HPLC-purified **2** indicated a molecular weight of 208. Metabolite **2** converted on standing to a compound whose FD mass spectrum indicated a molecular weight of 224, with chromatographic properties similar to those of 2,3,3-trichloro-2-propenesulfonic acid (**3**). These results suggested that **2** was the readily air-oxidized 2,3,3-trichloro-2-propenesulfinic acid. Reaction of metabolite **2** with methyl iodide in aqueous ethanol cleanly afforded methyl sulfone derivative **6**. The GC/EI mass spectrum of **6** displayed a weak molecular ion at m/z 222, consistent with the assigned structure. The mass spectrum of methyl sulfone **6** derived from metabolite **2** was essentially identical to that of synthetic **6**, except for the distribution of isotopically labeled ion peaks. Metabolite **2** appears to be the first alkylsulfinic acid reported as a xenobiotic animal metabolite. The observation of **2** as a metabolite was confirmed by synthesis via a novel method (see Discussion).

Metabolite 3 (2,3,3-Trichloro-2-propenesulfonic Acid). Metabolite **3** migrated on HVE toward the anode at pH 1.0, as expected of a strong acid. ^{13}C NMR analysis of the metabolite provided a chemical shift of 56.5 ppm for the ^{13}C-enriched C-1 carbon atom, the same value as found for synthetic **3**. Radiolabeled metabolite **3** coeluted with synthetic **3** on HPLC, and its methyl ester derivative **3a** coeluted with synthetic **3a**.

Metabolite 4 [1-Deoxy-1-[(2,3,3-trichloro-2-propenyl)thio]-β-D-glucopyranuronic Acid]. Metabolite **4** displayed an HPLC retention time of 9.5 min, and diazomethane afforded a methyl ester **4a** with a retention time of 11.1 min. Treatment of **4a** with acetic anhydride/pyridine gave a triacetate **4b** with a retention time of 16.3 min. Analysis of **4b** by direct-probe EI MS revealed a chlorine isotope ion cluster based at m/z 372, consistent with the loss of two acetic acid molecules. The direct-probe CI mass spectrum of derivative **4b** showed no chlorine isotope ions, but the base peak at m/z 317 was consistent with loss of 2,3,3-trichloro-2-propenethiol. The structure of metabolite **4** was confirmed by synthesis of triacetate **4b** starting from D-glucurone (Materials and Methods). Synthetic and metabolite-derived **4b** had matching chromatographic properties and gave comparable mass spectra except for differences in isotope ions and the absence of a molecular ion for metabolite-derived **4b**, whereas synthetic **4b** afforded a more intense mass spectrum featuring a weak molecular ion. The ^1H NMR spectrum of synthetic ester **4a** indicated a β-anomeric (equatorial) configuration for the thiol moiety.

Metabolite 5 [1,1,2-Trichloro-3-(methylsulfinyl)-1-propene]. The trace metabolite **5** was not stable to GC analysis. The direct-probe EI mass spectrum of **5** showed a molecular ion cluster centered at m/z 206 (^{13}C and Cl isotopes) and a similar cluster at m/z 190 arising via loss of an oxygen atom. The direct-probe CI mass spectrum featured an $[M + H]^+$ ion at m/z 207, which underwent loss of HCl to give an ion at m/z 171. These data were consistent with a methyl sulfoxide structure for metabolite **5**.

Metabolite 6 [1,1,2-Trichloro-3-(methylsulfonyl)-1-propene]. The methyl sulfone **6**, also a trace metabolite in excreta, provided satisfactory GC/MS data consistent with the assigned structure. The mass spectral and chromatographic properties of metabolite **6** and synthetic **6** were in excellent agreement.

Metabolite 7 [*N*-Acetyl-*S*-[2,2-dichloro-1-[(methylsulfonyl)methyl]ethenyl]-L-cysteine]. Treatment of metabolite **7** with diazomethane furnished methyl ester **7a**. The direct-probe CI mass spectrum of **7a** (ammonia) provided an $[M + NH_4]^+$ ion cluster at m/z 381, indicating a molecular weight of 363 for the ester, in good agreement with the highest molecular weight ion (m/z 363) observed in the direct-probe EI mass spectrum. The structure of **7a** was partially solved from high-resolution EI mass spectral data, which furnished a molecular formula of $C_{10}H_{15}NO_5S_2Cl_2$. The m/z 363 → 304 fragmentation represented a loss of CH_3CONH_2 and the m/z 304 → 225 fragmentation a loss of a CH_3SO_2 radical. These data suggested a structure with mercapturate conjugation to methyl sulfone **6**, but mass spectral data alone were insufficient to determine the location of the *N*-acetylcysteine moiety, necessitating structure confirmation by synthesis. Methyl sulfone **6** was a likely in vivo precursor of metabolite **7**, and synthetic **7** and its methyl ester **7a** were prepared in high yield by reaction of **6** with *N*-acetylcysteine (Materials and Methods). Synthetic **7** and **7a** displayed chromatographic properties identical with those of metabolite **7** and ester **7a**, as well as matching mass spectra, with the exception of isotopically labeled ion clusters.

The C-2 substitution in mercapturate **7** was verified by X-ray crystallographic analysis of crystalline synthetic **7** (Figure 3). Crystals of **7** belonged to a monoclinic lattice system with unit cell parameters of a = 13.368(2) Å, b = 7.5892(9) Å, c = 29.093(4) Å, and b = 94.47(1) Å, in symmetry group C_2. A single asymmetric unit contained two molecules of **7** and one water molecule. The structure was solved by Patterson heavy-atom methods and was refined by a full matrix least-squares procedure to a discrepancy factor of 0.059.

Metabolite 8 [2,2′-Thiobis[1,1-dichloro-3-(methylsulfonyl)-1-propene]]. Trace metabolite **8** was unstable to GC analysis and immobile on HVE, while diazomethane treatment caused no change in HPLC. The direct-probe CI mass spectrum showed an $[M + H]^+$ ion at m/z 407, while the heaviest ion in the direct-probe EI mass spectrum appeared at m/z 406. High-resolution EI mass spectral data provided a molecular formula of $C_8H_{10}O_4S_3Cl_4$ and featured the following transformations: 406 → 327, loss of CH_3SO_2; 327 → 264, loss of CH_3SO; 406 → 213, loss of Cl and two CH_3SO_2 fragments. These data were consistent

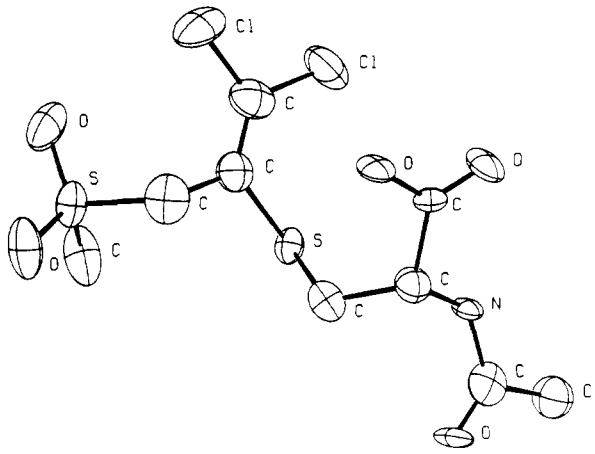

Figure 3. X-ray crystal structure of 7, with ellipsoids depicting non-hydrogen atoms.

with a dimeric sulfide structure for 8, with sulfur attachment at C-2 by analogy with metabolite 7, whose structure was proven by X-ray crystallography.

Metabolite 9 [3-[[[Bis(1-methylethyl)amino]carbonyl]thio]-2-chloro-2-propenoic Acid]. The 2-chloroacrylate 9, the first metabolite formed via the carbon oxidation pathway, was a minor component of excreta. On HVE 9 was mobile at pH 5.9 but not at pH 2.0, consistent with a carboxylic acid structure. Diazomethane treatment afforded a methyl ester **9a**, less polar than 9 on reversed-phase HPLC and having a GC retention time (relative to triallate) of 1.19. GC/CI mass spectral analysis of **9a** showed an $[M + H]^+$ ion cluster based at m/z 280, with isotope ion ratios consistent with ^{13}C and one chlorine atom. The GC/EI mass spectrum of metabolite 9 displayed the heaviest ion peak at m/z 152. This and other peaks in the GC/EI mass spectrum were consistent with the 2-chloroacrylate structure proposed for 9. A trans double-bond geometry was assigned by analogy with the structure of the 2-chloroacrylate metabolite 10.

Metabolite 10 [(*Z*)-*S*-(2-Carboxy-2-chloroethenyl)-L-cysteine]. Of the three 2-chloroacrylate metabolites in the C-oxidation pathway, 10 was the most abundant. Treatment of 10 with diazomethane afforded an ester **10a** with a longer HPLC retention time (5.4 → 8.3 min). Treatment of **10a** with acetic anhydride/pyridine furnished an acetate derivative **10b** with an HPLC retention time of 11.4 min. Metabolite 10 was amphoteric on HVE, moving toward the anode at pH 5.9 and toward the cathode at pH 1.0. The ^{13}C NMR spectrum of 10 displayed a ^{13}C-enriched carbon resonance at 136.6 ppm (Table II), which was a doublet in the off-resonance mode, consistent with location in a double bond and attachment to a single proton. The direct-probe CI mass spectrum of acetate derivative **10b** displayed an $[M + H]^+$ ion at m/z 296, with isotope ion ratios suggesting a single chlorine atom. MS, HVE, and ^{13}C NMR evidence supported the structure **10b** but were insufficient to determine the double-bond geometry and position of thiol attachment.

The acetylated 2-chloroacrylate **10c** was synthesized (Materials and Methods) and found to be spectroscopically and chromatographically indistinguishable from metabolite-derived **10c**. The structure of **10c** was confirmed by X-ray crystallography (Figure 4). Synthetic **10c** crystallized in an orthorhombic lattice system with unit cell parameters a = 6.059 Å, b = 10.348(2) Å, c = 17.837(4) Å, z = 4 Å, in space group $P2_12_12_1$. The structure was solved by direct methods and was refined by a least-squares procedure to a discrepancy factor of 0.046. Structure **10c**

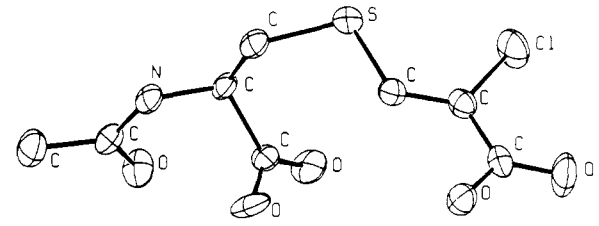

Figure 4. X-ray crystal structure of 10c, with ellipsoids depicting non-hydrogen atoms.

possesses a trans configuration of the carboxyl and sulfide moieties about the double bond, and the same configuration was assigned by analogy to the other 2-chloroacrylate metabolites 9 and 11.

Metabolite 11 [(*Z*)-3-[(Carboxymethyl)thio]-2-chloro-2-propenoic Acid]. Metabolite 11 migrated on HVE toward the anode at pH 5.9 and was immobile at pH 1.0, indicative of a carboxylic acid. The ^{13}C NMR spectrum of 11 displayed a signal at 139.2 ppm and a doublet in the off-resonance mode, indicating a structural similarity to metabolite 13. Treatment of 11 with diazomethane produced the methyl ester **11a**, which displayed a GC/EI mass spectrum with a prominent molecular ion cluster at m/z 224 and isotope ion ratios consistent with the presence of one chlorine atom. High-resolution EI mass spectral analysis provided the formula $C_7H_9O_4SCl$ and showed the following transformations: 224 → 192 → 160 (loss of methanol) and 224 → 151 (loss of $CH_2CO_2CH_3$). Synthetic 11 (Materials and Methods) displayed chromatographic and spectroscopic properties matching those of metabolite 11. By analogy with **10c**, the sulfide moiety of 11 was assigned a trans configuration relative to the carboxyl group.

Metabolite 12 (2,3,3-Trichloro-2-propenol). The GC and HPLC chromatographic properties of synthetic 12 and metabolite-derived 12 were in close agreement, and the GC/EI mass spectral analyses were virtually identical except for the presence or absence of ^{13}C isotope ions.

Metabolite 13 [*S*-(2,3,3-Trichloro-2-propenyl) (2-Hydroxy-1-methylethyl)(1-methylethyl)carbamothioate]. Metabolite 13 was HVE-immobile and did not form a derivative on treatment with diazomethane. However, 13 did react with acetic anhydride/pyridine to form an acetate **13a** with a longer retention time (16.1 → 18.6 min). Both 13 and **13a** were GC-stable, and 13 displayed a GC retention time relative to triallate of 1.26. The GC/CI mass spectrum of acetate 13 showed an $[M + H]^+$ ion at m/z 362 and a large ion at m/z 302, indicating the loss of acetic acid. The direct-probe EI mass spectrum of 13 showed a molecular ion cluster based at m/z 319, with chlorine isotope ion ratios characteristic of three chlorine atoms. The GC/EI and high-resolution EI mass spectra of **13a** demonstrated that the acetoxy group (and therefore the hydroxyl group of 13) was attached to a methylene carbon. High-resolution experiments indicated a loss of CH_2OCOCH_3 radical to form an acyliminium cation (m/z 287.9795, theoretical = 287.9792). Such an α-cleavage reaction (see supplementary material) would be expected for the primary alcohol/acetate structure assigned to 13 and **13a** (McLafferty, 1980). A second prominent high-resolution peak arises via extrusion of carbonyl sulfide from the initially formed α-cleavage product, followed by radical recombination to form a tertiary iminium cation (m/z 228.0120, theoretical = 228.0114), the latter also losing propylene to form a secondary iminium cation (m/z 186).

Metabolite Quantitation. HPLC-derived metabolite histogram data were combined with percentages of dose in excreta (Ridley et al., 1993) for calculation of metabolite

Table III. Triallate-Derived HPLC Radioactivity Distribution in Urine[a]

	5 mg/kg dose			500 mg/kg dose		
metabolite	males	females	av	males	females	av
2	20.3	22.5	21.4	17.5	16.3	16.9
3	4.9	2.6	3.8	1.5	1.3	1.4
4	0.3	0.3	0.3	3.2	4.0	3.6
5				0.7	0.9	0.8
6 + 12	0.7	0.9	0.8	0.7	0.9	0.8
7	3.6	6.8	5.2	6.9	10.6	8.8
8	0.3	0.3	0.3	0.3	0.3	0.3
9				0.4	0.6	0.5
10	1.1	1.5	1.3	2.8	3.2	3.0
11	0.8	1.4	1.1	2.2	2.1	2.2
total identified	32.0	36.3	34.2	36.2	40.2	38.2
unidentified[b]	11.8	13.6	12.7	6.8	9.6	8.2

[a] Expressed as percentage of dose. [b] Mixture of polar, low-level components.

Table IV. Triallate-Derived HPLC Radioactivity Distribution in Feces[a]

	5 mg/kg dose			500 mg/kg dose		
metabolite	males	females	av	males	females	av
1	2.1	1.9	2.0	8.1	4.7	6.4
2	7.0	4.6	5.8	3.2	3.0	3.2
3	3.0	1.6	2.3	1.0	0.8	0.9
4				0.7	0.6	0.7
7	2.4	2.4	2.4	1.8	2.1	2.0
9				0.1	0.2	0.2
10	2.7	2.0	2.4	2.4	2.2	2.3
11				0.7	0.5	0.6
13	0.1	0.1	0.1	0.4	0.2	0.3
total identified	17.3	12.6	15.0	18.6	14.3	16.5
unidentified[b]	16.5	11.9	14.2	13.5	11.5	12.5

[a] Expressed as percentage of dose. [b] Mixture of polar, low-level components.

Table V. Distribution of Triallate Metabolites According to Pathway of Formation[a]

	5 mg/kg dose			500 mg/kg dose		
metabolite[b]	males	females	av	males	females	av
S-oxidation pathway						
2	27.3	27.1	27.2	20.9	19.3	20.1
3	7.9	4.2	6.1	2.5	2.1	2.3
total	35.2	31.2	33.3	23.4	21.5	22.4
thiol pathway						
4	0.3	0.3	0.3	3.9	4.6	4.3
5				0.7	0.9	0.8
7	6.0	9.2	7.6	8.7	12.7	10.7
8	0.3	0.3	0.3	0.3	0.3	0.3
total	6.6	9.8	8.2	13.6	18.4	16.2
C-oxidation pathway						
9				0.5	0.8	0.7
10	3.8	3.5	3.7	5.2	5.4	5.3
11	0.8	1.4	1.1	2.9	2.6	2.7
13	0.1	0.1	0.1	0.4	0.2	0.3
$^{14}CO_2$	4.3	4.9	4.6	3.4	4.6	4.0
total	9.0	9.9	9.5	12.4	13.6	13.0

[a] Expressed as percentage of dose. [b] Excluding coeluted 6 and 12 (Table III), formed in different pathways, and triallate.

distributions as percentages of dose. Tables III and IV illustrate the levels of identified and unidentified metabolites in urine and feces, respectively. The largely polar unidentified radioactivity consisted of complex mixtures that resisted further attempts at identification. Since triallate rat metabolites appear to form along three distinct mechanistic pathways, metabolite distribution data for total excreta were also calculated according to route of formation. Table V illustrates metabolite levels arising via the S-oxidation, thiol, and C-oxidation pathways, respectively, in descending order of quantitative contribution to overall metabolite distribution. Table V also summarizes the $^{14}CO_2$ expiration observed in this study, which averaged 4.6% and 4.0% for the 5 and 500 mg/kg dose groups, respectively. Unchanged triallate was found only in feces and was excreted more readily at the 500 mg/kg dose level (Table IV), indicative of partial saturation of triallate catabolism above the 5 mg/kg dose level.

Table VI. Urinary Metabolites in Rats Dosed with Triallate Metabolites[a]

metabolite	dosed with 2[b]	dosed with 14[b]
2	23.1	1.0
3	9.1	<1.0
4	ND[c]	2.5
5	ND[c]	11.4

[a] Averaged over sexes and expressed as percentage of dose. [b] Dosed at 5 mg/kg. [c] Not detected in HPLC (<0.1%).

Demonstration of in Vivo Formation of Thiol 14. Identification of thioglucuronide 4 as a major rat metabolite suggested that cleavage of triallate in vivo could produce 2,3,3-trichloro-2-propenethiol (14) (Figure 1) as an intermediate in the formation of 4 and the sulfoxide/sulfone metabolites 5–8. We therefore decided to test sulfinic acid 2 and thiol 14 as potential precursors of metabolites 4–8 in separate administration to rats.

[1-^{14}C]-2,3,3-Trichloro-2-propenesulfinic acid (2) was orally dosed to rats in phosphate buffer. Two male rats and two female rats each received a dose corresponding to 5 mg/kg of radiolabeled sulfinic acid equivalents and were handled thereafter in a manner analogous to rats previously dosed with triallate (Ridley et al., 1993), except that expired air was not collected to detect $^{14}CO_2$. Males excreted an average of 69% of the dosed radioactivity within 72 h (51% via urine and 18% via feces), while females excreted an average of 85% of the dosed radioactivity within 72 h (65% via urine and 20% via feces). For experimental simplicity, only urine was analyzed for excreted metabolites. The sulfinic acid 2 was recovered as the primary urinary constituent (23% of the dose for both sexes), and some sulfonic acid 3 was also isolated (9% of the dose). None of the thiol and methyl sulfone metabolites 4–8 was observed (Table VI).

[1-^{14}C]-2,3,3-Trichloro-2-propenethiol (14) was also orally administered to rats in corn oil. Two male rats and two female rats each received a dose corresponding to 5 mg/kg of radiolabeled thiol equivalents and were handled thereafter in a manner analogous to rats dosed with 2. Males excreted an average of 73% of the dosed radioactivity within 72 h (46% via urine and 27% via feces), while females excreted an average of 56% of the dosed radioactivity within 72 h (34% via urine and 22% via feces). The methyl sulfone mercapturate 7 was recovered as the primary urinary metabolite (11% of the dose for both sexes), and 4 was also isolated from urine (2.5% of the dose). Only very small amounts of sulfinic acid 2 (1% of dose) and sulfonic acid 3 (<1% of dose) were detected in urine (Table VI), indicating that thiol 14 was not a precursor of the sulfur acid metabolites in vivo.

DISCUSSION

S-Oxidation Pathway. S-Oxidation of triallate, leading to sulfinic acid 2 and sulfonic acid 3, represents the primary route of triallate metabolism in rats. This is an important finding, since both sulfur acids are highly water-soluble and readily excreted and since sulfonic acid 3 is metabolically inert (Hackett et al., 1993). Although sulfinic acid 2 is the major metabolite of triallate in rats and is also readily formed in vitro (Hackett et al., 1993), there have

Scheme I

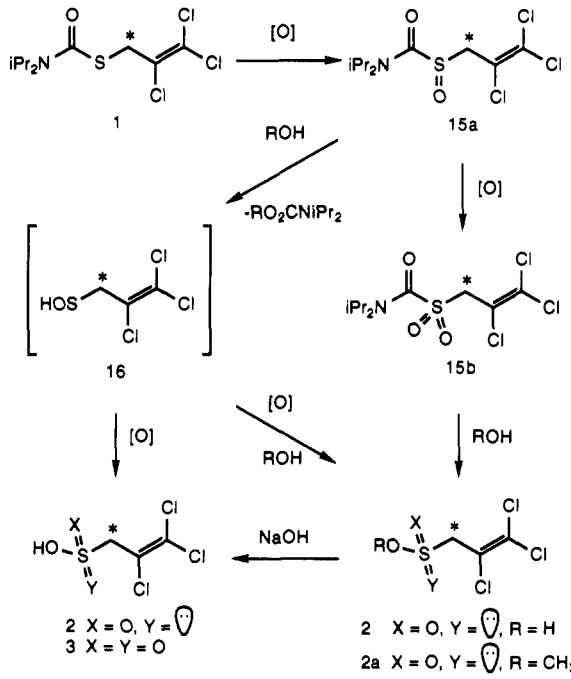

Scheme II

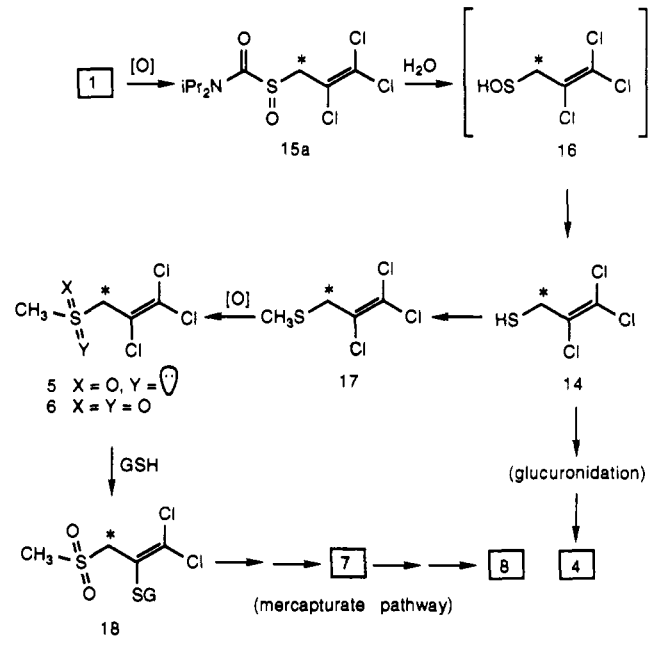

been no previous reports of **2** as an in vivo or in vitro metabolite in other triallate metabolism studies (Mair and Casida, 1991). As far as we are aware, metabolite **2** is the first reported sulfinic acid derived from a xenobiotic. Sulfonic acid **3** (TCPSA) has been previously reported as a major triallate plant metabolite (Ebing and Schuphan, 1979).

S-Oxidation of thiocarbamate herbicides to sulfoxides has been proposed as a mechanism of bioactivation (Chen et al., 1979; Schuphan and Casida, 1979; Hubbell and Casida, 1977; Casida et al., 1975), and thiocarbamate sulfoxides have been shown to react with thiols in vitro to give transcarbamoylation products and sulfenic acids (Lay et al., 1975). In this study both sulfinic acid **2** and sulfonic acid **3** likely arise via S-oxidation of triallate, followed by hydrolysis and further oxidation (Scheme I). The intermediacy of **14** in the formation of **2** and **3** (Figure 1) appears to be excluded by the demonstration that rats dosed orally with [^{14}C]thiol **14** did not excrete significant amounts of the sulfinic acid **2** in their urine. Triallate therefore appears to undergo oxidation at sulfur as an activation step for sulfinic acid formation. Our experiments do not distinguish whether sulfinic acid **2** forms via cleavage of triallate sulfoxide **15a** and oxidation of sulfenic acid **16** (Scheme I) or via formation of triallate sulfone **15b**, followed by hydrolysis.

The rationale for our novel synthesis of sulfinic acid **2** by oxidation of triallate was suggested by the postulated S-oxidation pathway for the in vivo conversion of triallate to **2**. Attempts to prepare **2** using conventional methods (Stirling, 1971), such as reduction of the sulfonyl chloride derived from sulfonic acid **3**, were unsuccessful. Literature searching disclosed no examples of sulfinic acid synthesis by S-oxidation of a thiocarbamate or other thiocarbonyl compound. Initial attempts to oxidize triallate to **2** resulted in low yields of the desired product. We determined that methyl sulfinate ester **2a** (Figure 1) could be formed in good yield using equimolar sodium periodate and triallate in methanolic HCl and that **2a** could be converted to **2** by controlled alkaline hydrolysis. The formation of a methyl sulfinate ester **2a** can proceed via attack of methanol at the carbonyl group of sulfoxide **15a**, followed by oxidation/esterification of the initially formed sulfenic acid **16** (Scheme I), or via solvolysis of triallate sulfone **15b**, followed by esterification of **2**.

Thiol Formation and Reactions. The formation of polar, readily excreted derivatives of 2,3,3-trichloro-2-propenethiol (**14**) constitutes the second most important route of triallate rat metabolism. Although **14** was not detected in excreta of rats dosed with triallate, the identification of thiol-derived metabolites provided strong evidence for the formation of **14** as a metabolic intermediate. Thiol **14** most likely arises via reduction or disproportionation of the sulfenic acid **16** formed by triallate S-oxidation and hydrolysis (Scheme II). Sulfenic acid–thiol interconversion is well precedented (Allison, 1976). Two reactions appear to compete for transformation of **14**: S-glucuronidation and S-methylation (Scheme II). S-Glucuronidation of thiol **14** leads to thioglucuronide **4**, a major in vivo metabolite whose formation is well precedented (Larsen and Bakke, 1978; Clapp, 1956).

S-Methylation of **14** leads (Scheme II), by way of the methyl sulfide **17** (not isolated), to the sulfoxide **5** (trace metabolite), sulfone **6** (trace metabolite), and mercapturate **7** (major metabolite). Thiol methylations are known to occur in transformations of mercapturate breakdown products of xenobiotics (Sharp, 1990; Borchardt and Cheng, 1977). The mercapturate **7** is the second most abundant metabolite found in the excreta of both low-dose and high-dose rats and presumably originates via glutathione conjugation of sulfone **6**, followed by catabolism of the resulting conjugate **18** via the mercapturic acid pathway (Bakke, 1986). The dimeric sulfide trace metabolite **8** likely arises via formation of a C-2-substituted thiol as a breakdown product in the mercapturate pathway, followed by reaction of the latter with a second equivalent of metabolite **6**, by analogy with the formation of **18** (Scheme II).

The apparent formation of metabolite **7** via initial reaction of glutathione with methyl sulfone **6** suggested a synthetic route to **7**. Synthetic **6** was obtained by reaction of 1,2,3,3-tetrachloropropene with sodium methyl sulfinate (Materials and Methods). *N*-Acetylcysteine underwent smooth reaction with **6** at pH 9, and the product **7** was identical to the metabolite by MS, NMR, and HPLC analysis. The structure of synthetic **7** was proven unambiguously by X-ray crystallography (Figure 3).

Scheme III

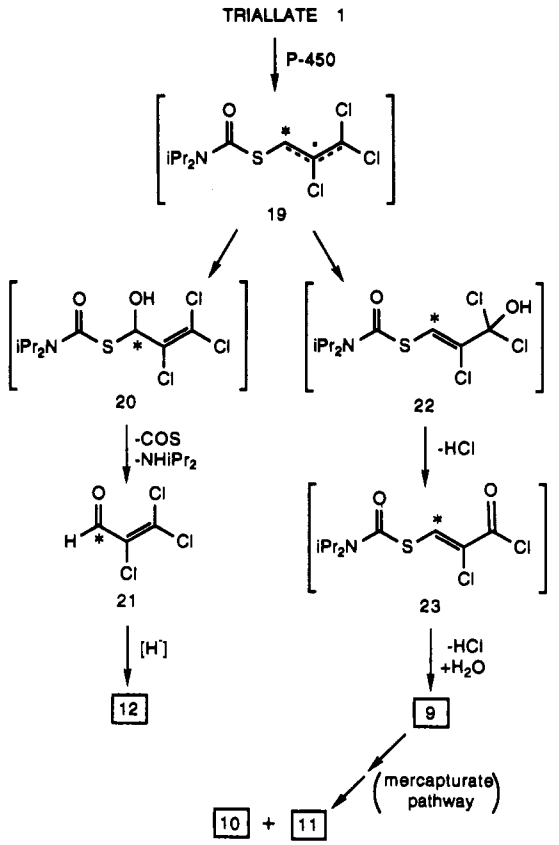

Dosing experiments carried out with sulfinic acid 2 and thiol 14 demonstrated the intermediacy of 14 in the formation of thioglucuronide 4 and the metabolites 5–8 (Scheme II). The presence of thiol-derived metabolites in the urine of rats dosed orally with thiol 14, and their absence from the urine of rats dosed orally with sulfinic acid 2, strongly supports the postulated metabolic intermediacy of 14 rather than 2 in the formation of these metabolites. On the other hand, the meager amounts of sulfinic acid 2 and sulfonic acid 3 in the urine of thiol-dosed rats indicate that these metabolites form *after* an initial sulfur oxidation of triallate itself, rather than via the intermediacy of thiol 14.

Carbon Oxidation Pathway. In contrast to the central role of sulfur oxidation, we have found that the formation of C-oxidation products represents a secondary route for triallate degradation in vivo. Hydroxytriallate 13, a minor rat metabolite, arises via hydroxylation of the diisopropylamine moiety of triallate. Other minor triallate metabolites can be rationalized as arising via oxidation reactions occurring at either the C-1 or C-3 carbon atoms of triallate. Trichloroallyl alcohol 12 is likely to arise via hydroxylation at the C-1 allylic position (Scheme III), followed by reduction of the intermediate trichloroacrolein 21 (Hackett et al., 1990).

Cytochrome P-450 activation of triallate at the C-1 position would generate an enzyme-bound intermediate represented in Scheme III as an allylic radical species 19 (Guengerich and Macdonald, 1990). Hydroxylation of the latter at the C-3 position would lead via 22 and 23 to the 2-chloroacrylate 9. Either alcohol 22 or metabolite 9 could serve as precursors for the glutathione-derived metabolites 10 and 11 (Figure 1) via conjugate addition of glutathione, followed by further transformations in the mercapturic acid pathway (Bakke, 1986). These possibilities have been separately addressed in the following paper (Hackett et al., 1993). The alcohol 22 could also arise via a formal S_N2'-type rearrangement of initially formed intermediate 20, although harsh conditions are normally required for such rearrangements (Kruper and Emmons, 1991).

Metabolite Distribution. Rats dosed with triallate did not exhibit major gender-related differences in the level and distribution of excreted metabolites, although females tended to eliminate more of the dose in urine and less in feces, as compared with males (Tables III and IV). Metabolites in the S-oxidation pathway, i.e., 2, constituted the largest fraction of identified triallate metabolites (Table V) and were excreted largely in urine, as opposed to feces. This was the case for both sexes at both dose levels. However, animals in the high-dose groups (500 mg/kg) excreted a higher fraction of the dose via thiol-derived and C-oxidized metabolites, indicating relative saturation of the S-oxidation pathway at the higher dose level.

Metabolites derived from thiol 14 constituted the second largest fraction of excreted triallate metabolites (Table V). The methyl sulfone mercapturate 7 was the second most abundant metabolite in both sexes at both dose levels and was excreted in urine and feces. Other thiol-derived metabolites, in particular thioglucuronide 4, were excreted to an appreciable extent only at the higher dose level. The separate feeding study conducted with radiolabeled sulfinic acid 2 and thiol 14 demonstrated that 2 does not act as a significant precursor of thiol pathway metabolites and that 14 does not act as significant precursor of the sulfur acids 2 and 3.

Metabolites belonging to the carbon oxidation pathway constituted the smallest fraction of triallate metabolites identified in excreta at both dose levels (Table V). Metabolites in this pathway were excreted at higher levels in the high-dose groups, in contrast to the lowered relative output via the S-oxidation pathway at the high dose. This observation may be important for interpreting toxicological responses at high feeding levels, since mutagenic metabolites are believed to arise via the C-oxidation pathway (Mair and Casida, 1991).

Formation of Expired $^{14}CO_2$. Rats produce $^{14}CO_2$ from [^{14}C]triallate (Table V). Males and females expired similar fractions of the dose as $^{14}CO_2$ at each dose level, although each sex expired a somewhat higher fraction of the dose as $^{14}CO_2$ at the low dose as compared with the high dose. The latter observation indicates some saturation of $^{14}CO_2$ formation at the 500 mg/kg dose level. The mechanism of $^{14}CO_2$ is unknown, although one or more metabolites in the C-oxidation pathway may be broken down at the C-1 position to release $^{14}CO_2$. Intermediates in $^{14}CO_2$ release might also be expected to participate in some radiolabel incorporation into natural products.

Conclusions. Triallate metabolism in rats displays features in common with transformations of other thiocarbamate herbicides, as well as significant differences. The metabolism of triallate to readily excreted sulfur acids and 2,3,3-trichloropropenethiol derivatives is noteworthy and represents the primary route of degradation. The structures of identified triallate metabolites indicate that metabolism in rats proceeds via three main pathways, i.e., S-oxidation leading to sulfur acids, S-oxidation/hydrolysis/reduction leading to thiol derivatives, and C-oxidation of the 2,3,3-trichloropropenethiol moiety. Excretion patterns after administration of radiolabeled 2,3,3-trichloropropenethiol and 2,3,3-trichloropropenesulfinic acid confirm the thiol as a precursor of metabolites with an unoxidized sulfur atom. Sulfur acid formation was more important at the 5 mg/kg dose rate, while thiol production and carbon oxidation gained in significance at the 500 mg/kg rate,

consistent with saturation of the S-oxidation pathway. Unchanged triallate was also excreted at the 500 mg/kg dose level, consistent with saturation of uptake and/or metabolism. Elevated excretion of triallate and C-oxidation metabolites should be considered in interpreting high-dose triallate feeding studies, since mutagenic effects have been ascribed to products of the C-oxidation pathway.

ACKNOWLEDGMENT

We thank Dr. Robert C. Freeman and Mr. Brent V. Mischke for providing us with samples of isotopically labeled triallate, Ms. JoAnne Warren for the husbandry of animals dosed with triallate metabolites, and Dr. William R. Ridley for his advice and suggestions.

Supplementary Material Available: Detailed preparation of **4a**, **6**, **7**, **10c**, and **11**, fragmentation scheme for mass spectrum of **13a**, and table of mass spectral data for triallate metabolites and derivatives (6 pages). Ordering information is given on any current masthead page.

LITERATURE CITED

Allison, W. S. Formation and Reactions of Sulfenic Acids in Proteins. *Acc. Chem. Res.* **1976**, *9*, 293–299.

Bakke, J. E. Catabolism of Glutathione Conjugates. In *Xenobiotic Conjugation Chemistry*; Paulson, G. D., Caldwell, J., Hutson, D. H., Menn, J. J., Eds.; ACS Symposium Series 299; American Chemical Society: Washington, DC, 1986; pp 301–321.

Borchardt, R. T.; Cheng, C. F. Purification and Characterization of Rat Liver Microsomal Thiol Methyltransferase. *Biochim. Biophys. Acta* **1978**, *522*, 340–353.

Bowering, W. D. S.; Timell, T. E. Synthesis and Characterization of 2-O-(β-D-Glucopyranosyluronic acid)-D-xylopyranose. *J. Am. Chem. Soc.* **1960**, *82*, 2827–2830.

Casida, J. E.; Gray, R. A.; Tilles, H. Thiocarbamate Sulfoxides. Potent, Selective, and Biodegradable Herbicides. *Science* **1974**, *184*, 573–574.

Casida, J. E.; Kimmel, E. C.; Ohkawa, H.; Ohkawa, R. Sulfoxidation of Thiocarbamate Herbicides and Metabolism of Thiocarbamate Sulfoxides in Living Mice and Liver Enzyme Systems. *Pestic. Biochem. Physiol.* **1975**, *5*, 1–11.

Chen, Y. S.; Schuphan, I.; Casida, J. E. S-Chloroallyl Thiocarbamate Herbicides: Mouse hepatic Microsomal Oxygenase and Rat Metabolism of *cis*- and *trans*-[^{14}C=O]Diallate. *J. Agric. Food Chem.* **1979**, *27*, 709–712.

Clapp, J. W. A New Metabolic Pathway for a Sulfonamide Group. *J. Biol. Chem.* **1956**, *223*, 207–214.

DeBaun, J. R.; Bova, D. L.; Chien, T. K.; Menn, J. J. Metabolism of [ring-^{14}C]Ordram (Molinate) in the Rat. 2. Urinary Metabolite Identification. *J. Agric. Food Chem.* **1978**, *26*, 1098–1104.

Ebing, W.; Schuphan, I. In *Herbizide*; Boerner, H., Heitefuss, R., Hurle, K., Eds.; Harold Boldt Verlag: Boppard, Germany, 1979; pp 112–126.

Guengerich, F. P.; Macdonald, T. L. Mechanisms of Cytochrome P-450 Catalysis. *FASEB J.* **1990**, *4*, 2453–2459.

Hackett, A. G.; Fujiwara, H.; Kotyk, J. J.; Logusch, E. W. Identification of a Unique Glutathione Conjugate of Trichloroacrolein Using Heteronuclear Multiple Quantum Coherence ^{13}C Nuclear Magnetic Resonance Spectroscopy. *J. Am. Chem. Soc.* **1990**, *112*, 3669–3671.

Hackett, A. G.; Fujiwara, H.; Kotyk, J. J.; Logusch, E. W. Metabolism of Triallate in Sprague-Dawley Rats. 3. In Vitro Metabolic Pathways. *J. Agric. Food Chem.* **1993**, third of three papers in this issue.

Hubbell, J. P.; Casida, J. E. Metabolic Fate of the *N,N*-Dialkyl Moiety of Thiocarbamate Herbicides in Rats and Corn. *J. Agric. Food Chem.* **1977**, *25*, 404–413.

Kruper, W. J., Jr.; Emmons, A. H. Transformations of the Trichlorovinyl Group: Synthesis of α-Halocinnamate Esters from Aryltrichlorovinyl Ketones. *J. Org. Chem.* **1991**, *56*, 3323–3329.

Larsen, G. L.; Bakke, J. E. Mass Spectral Characterization of the Glucuronide Conjugates of Terbutyrn [2-(*t*-Butylamino)-4-ethylamino)-6-(methylthio)-5-triazine] Metabolites from Rats and Goats. *Biomed. Mass Spectrom.* **1978**, *5*, 391–394.

Lay, M. M.; Hubbell, J. P.; Casida, J. E. Dichloroacetamide Antidotes for Thiocarbamate Herbicides. Mode of Action. *Science* **1975**, *189*, 287–289.

Leonard, N. J.; Johnson, C. R. Periodate Oxidation of Sulfides to Sulfoxides; Scope of the Reaction. *J. Org. Chem.* **1962**, *27*, 282–284.

Mair, P.; Casida, J. E. Diallate, Triallate and Sulfallate Herbicides: Identification of Thiocarbamate Sulfoxides, Chloroacroleins, and Chloroallylthiols as Mouse Microsomal Oxidase and Glutathione *S*-Transferase Metabolites. *J. Agric. Food Chem.* **1991**, *39*, 1504–1508.

Marsden, J. M.; Casida, J. E. 2-Haloacrylic Acids as Indicators of Mutagenic 2-Haloacrolein Intermediates in Mammalian Metabolism of Selected Promutagens and Carcinogens. *J. Agric. Food Chem.* **1982**, *30*, 627–631.

McLafferty, F. W. *Interpretation of Mass Spectra*; University Science: Mill Valley, CA, 1980; p 51.

Ridley, W. P.; Warren, J. A.; Nadeau, R. G. Metabolism of Triallate in Sprague-Dawley Rats. 1. Material Balance, Tissue Distribution, and Elimination Kinetics. *J. Agric. Food Chem.* **1993**, first of three papers in this issue.

Schuphan, I.; Casida, J. E. [2,3]Sigmatropic Rearrangement of *S*-(3-Chloroally)thiocarbamate Sulfoxides Followed by a 1,2-Elimination Reaction Yielding Aldehydes and Acid Chlorides. *Tetrahedron Lett.* **1979**, *10*, 841–844.

Sharp, D. B. Alachlor. In *Herbicides: Chemistry, Degradation and Mode of Action*; Kearney, P. C., Kaufman, D. D., Eds.; Dekker: New York, 1988; pp 301–333.

Stirling, C. J. M. Sulfinic Acids and Their Derivatives. *Int. J. Sulfur Chem.* **1971**, *6B*, 277–320.

Received for review April 27, 1992. Revised manuscript received September 22, 1992. Accepted October 5, 1992.